A tangentially viewing fast ion D-alpha diagnostic for NSTX[a)]

A. Bortolon,[1,b)] W. W. Heidbrink,[1] and M. Podestà[2]
[1]*University of California, Irvine, California 92697, USA*
[2]*Princeton Plasma Physics Laboratory, Princeton, New Jersey 08543, USA*

(Presented 18 May 2010; received 17 May 2010; accepted 3 September 2010; published online 25 October 2010)

A second fast ion D-alpha (FIDA) installation is planned at NSTX to complement the present perpendicular viewing FIDA diagnostics. Following the present diagnostic scheme, the new diagnostic will consist of two instruments: a spectroscopic diagnostic that measures fast ion spectra and profiles at 16 radial points with 5–10 ms resolution and a system that uses a band pass filter and photomultiplier to measure changes in FIDA light with 50 kHz sampling rate. The new pair of FIDA instruments will view the heating beams tangentially. The viewing geometry minimizes spectral contamination by beam emission or edge sources of background emission. The improved velocity-space resolution will provide detailed information about neutral-beam current drive and about fast ion acceleration and transport by injected radio frequency waves and plasma instabilities. © *2010 American Institute of Physics.* [doi:10.1063/1.3495768]

I. INTRODUCTION

In the frame of tokamak research, the study of the interaction between fast ions (ions of energy much larger than ion temperature) and radio frequency (rf) waves or plasma instabilities requires accurate experimental knowledge of the fast ion distribution function. Fast ion D-alpha (FIDA) diagnostics obtain such information from the spectroscopic study of the deuterium Balmer α line ($n=3\rightarrow 2$, $\lambda=656.1$ nm), emitted by fast ions after charge exchange (CX) recombination with neutral atoms.[1] In the plasma core, neutral donors are typically provided by heating neutral beams (NBs), which often are also the major source of suprathermal ions with energies of tens of keV. At these energies, the Doppler shifted D_α spectrum extends to wavelengths out of the range dominated by cold emission from the plasma edge and beam emission. The analysis of these "hot tails" provides the information on the fast ion population.

The principle of the FIDA technique and examples of its implementation are discussed in detail in a recent review.[2] A crucial aspect is the effective average over velocity-space that is a characteristic of each diagnostic setup and is mainly determined by the viewing geometry relative to the neutral beam and magnetic field.[3] The sensitivity to different portions of the fast ion velocity-space can be expressed by the weight function $W_\lambda(E,p)$ (mapped in energy E and pitch angle $p=v_\parallel/v$ coordinates, where v is the fast ion velocity and $v_\parallel$ its component parallel to magnetic field). The measured FIDA spectrum $s(\lambda)$, apart from numerous background components, results from the convolution of $W_\lambda(E,p)$ with the fast ion distribution function $F(p,E)$,

$$s(\lambda)=\int W_\lambda(p,E)F(p,E)dEdp. \quad (1)$$

Since its installation in 2008, a FIDA diagnostic[4] has been extensively used on NSTX to address, e.g., fast ion acceleration[5] due to rf or their interaction with Alfvén modes.[6,7] Due to the quasivertical view, the present diagnostic is sensitive to fast ions with large velocity in the direction perpendicular to magnetic field B; hence, it is sensitive to the $p\sim 0$ region of phase space. On the other hand, NSTX fast ions originate from ionization of NB neutrals that are injected tangentially in the cocurrent direction. Thus, the majority of fast ions are expected to have $p\gtrsim 0.5$.

In this paper, we present the design of a new FIDA system for NSTX, with a view tangential to the B field (t-FIDA). The new t-FIDA system will complement the existing one by sampling more efficiently the parallel part of distribution function. This is illustrated in Fig. 1, where the response function $W_\lambda(E,p)$ of the present vertical view and the proposed tangential diagnostic are compared at sample wavelength $\lambda=652.12$ nm, corresponding to photons of energy $E_\lambda=35$ keV.[8] The results in the figure refer to a measurement at major radius $R=1.2$ m (normalized minor radius of $r/r_{max}\approx 0.35-0.45$ in NSTX typical plasma shapes). The t-FIDA response has a sharp peak in the $p>0.8$, $35<E<40$ keV region of velocity-space, confirming the enhanced sensitivity to the parallel part of the fast ion distribution function. Furthermore, the restricted range of energies contributing to the signal measured by tangential FIDA indicates that the effective averaging intrinsic to the technique will be less severe compared to vertical FIDA, resulting in an enhanced energy resolution.

The proposed t-FIDA will provide a tool to study the fast ion parallel dynamics (e.g., in the case of beam induced current drive) and to address the role of passing ($p\sim 1$) and trapped ($p\sim 0$) fast ions on turbulent or mode induced trans-

[a)]Contributed paper, published as part of the Proceedings of the 18th Topical Conference on High-Temperature Plasma Diagnostics, Wildwood, New Jersey, May 2010.
[b)]Electronic mail: abortolo@pppl.gov.

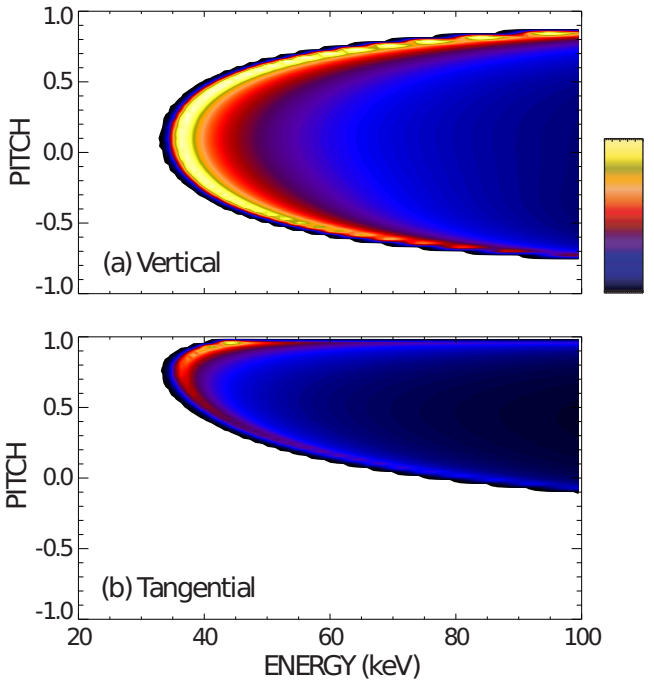

FIG. 1. (Color online) Response function $W_\lambda(E,p)$ for the present vertical FIDA (a) and the proposed tangential FIDA (b) for measurement at $R=1.2$ m and at $E_\lambda=35$ keV. Color scale is normalized to the maximum value.

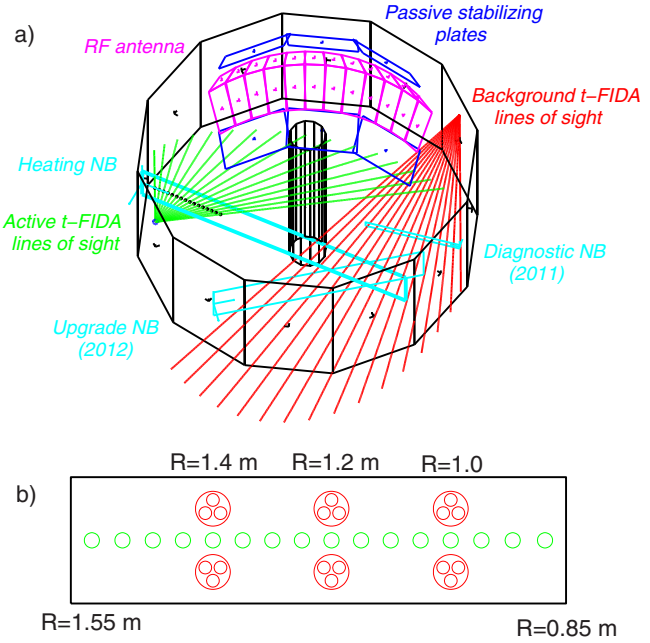

FIG. 2. (Color online) (a) Schematic representation of ts-FIDA observation geometry, showing the LOS for active (green) and background (red) view; the existing heating NB; the upgrade heating NB and diagnostic NB (cyan), planned for installation; passive stabilizing plates (blue); and rf antenna (magenta). (b) Fiber head configuration at the image plane of the collection lens, showing the array of 16 fibers dedicated to the spectroscopic measurement and the 6 bundles of 3 fibers dedicated to the filter measurement.

port. The t-FIDA diagnostic will be installed after the 2010 experimental campaign and is expected to be operational during the NSTX 2011 experimental run.

In the remainder of this paper, we describe the diagnostic layout (Sec. II), the issues connected to the choice of view location (Sec. III), and the expected performance (Sec. IV). The technical details of the main equipment elements can be found in the references.

II. DIAGNOSTIC SCHEME

As commonly found for active CX diagnostics, a lens[9] observing the heating neutral beam [Fig. 2(a)] focuses the plasma emission onto a number of optical fibers.[10] Each fiber collects light along a different line of sight (LOS) and the intersection between the LOS and the beam determines the localization of the measurement. In the present design, the selected collection lens (focal length of 20 mm, F/1.7) covers the 56° field of view with magnification of 35–40. The diameter of each emitting volume is ≈20 mm compared with 8 mm for the vertical system. Note that the increased radial size of emitting volumes does not compromise the spatial resolution of the instrument, which is limited to 30–50 mm due to (1) the large fast ion gyroradius, (2) the radial extension of emitting volumes, and (3) the mean free path of $n=3$ excited deuterons.

Since the FIDA spectrum is generally less intense than the bright background composed by line and bremsstrahlung emission, background evaluation is a key aspect of the measurement. For this purpose, t-FIDA will rely on a duplicate view missing the beam.

The presently installed FIDA diagnostic consists of a spectroscopic instrument (s-FIDA) plus a filter-based instrument (f-FIDA).[4] The proposed tangential FIDA replicates the same scheme, with similar designs for the two systems.

For the energy resolved measurement (ts-FIDA), part of the fibers transfer the light to a high throughput spectrometer[11] that uses a high dispersion holographic grating to select a spectral band of ≈30 nm centered on the D_α rest wavelength. At the output image plane, a narrow neutral density filter attenuates the cold D_α peak, which otherwise dominates the spectrum. Finally, a demagnification system projects the image of the filtered spectrum on a high quantum efficiency CCD.[12] By using a double curved slit at the spectrometer entrance, 16+16 (active+background) channels can be imaged on the detector in two vertically aligned arrays. A band pass filter at the spectrometer entrance avoids the cross-talk of the adjacent spectra.

The rest of the fibers will be dedicated to a filter-based measurement (tf-FIDA), as in the present f-FIDA.[4] In this case, the light coming from a given radial location is filtered by a narrow band pass filter ($\Delta\lambda \simeq 2$ nm) to a wavelength range virtually free from beam and impurity emission. The intensity of the filtered light is then measured by a photomultiplier tube (PMT).[13] Using a smaller spectral resolution, sample frequencies of 50 kHz are obtained.

Figure 2(b) shows a possible arrangement of the fiber heads at the image plane of the collection lens. This configuration optimizes the light input and allows the tangential systems to sample the same plasma volumes as the vertical instruments. The 16 spectroscopic measurements cover $R=0.85-1.55$ m. In most NSTX plasmas, the magnetic axis is located at $R=1.0-1.05$ m and the last closed flux surface at $R=1.45-1.55$ m; therefore, full radial coverage is guaran-

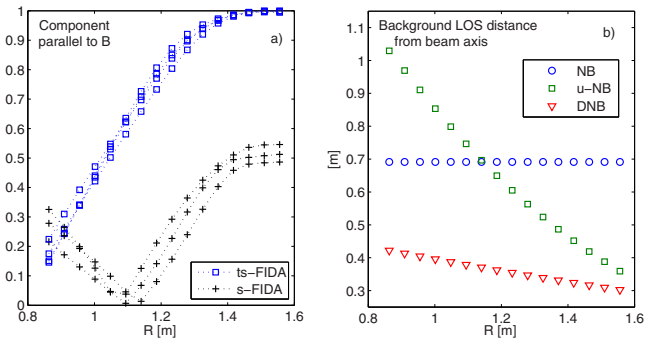

FIG. 3. (Color online) (a) Component of LOS vector parallel to the magnetic field at the measurement location, for the present s-FIDA (crosses), and the new ts-FIDA (squares). (b) Minimum distance between the background LOS and the different NB injection lines.

teed. For the filter measurement, three radial positions ($R=1.0$, 1.2, 1.4 m) are each sampled with six fibers, arranged in two bundles of three, to maximize photon statistic.

III. VIEW LOCATION

The location of collection optics is crucial for the diagnostic performance as it determines the response function $W_\lambda(E,p)$. Figure 2 shows the selected location of lenses for the active and background views. The first is positioned 30° from the NB entrance, 42 cm above the midplane. The second, with the same view angle, is toroidally displaced by ≈180°. This choice results from a compromise between diagnostic related constraints (e.g., minimize background light contamination) and machine related constraints (access, compatibility with future upgrades, etc.). In designing the tangential view, an effort has been made to maximize the projection of magnetic field on the line of sight at the emission volume location. In Fig. 3, the component of the LOS unit vector parallel to the magnetic field is shown at 16 measurement radii, evaluated for a set of NSTX discharges, representative of different NSTX plasma scenarios (maximum magnetic pitch angle is ≈30°–45°; edge safety factor is ≈8–15). The same quantity is shown for the present s-FIDA vertical view. The ts-FIDA parallel component is maximized in the outermost region of the plasma and decreases in the core to values that remain over 50% at $R=1$ m, where the magnetic axis is typically located. The parallel component of s-FIDA and ts-FIDA differ substantially along the low field side radius $R>1.0$ m. Here, they are expected to provide complementary information on the fast ion distribution function, i.e., to be characterized by a substantially different response function. Conversely, the innermost LOS, measuring at the high field side minor radius, will sample similar portions of the phase space and may be used to cross validate the measurement.

Another key point is that background channel LOS must avoid highly radiative, toroidally localized machine elements, such as limiters, rf antenna plates, or divertor plates, which may compromise accurate evaluation of the background emission. In the proposed configuration, all LOS views the first wall on passive stabilizing plates, which are covered by carbon tiles and uniformly distributed around the torus. This is expected to minimize contamination from stray light, e.g., from beam reflections on vessel elements. Moreover, because LOSs do not cross the divertor region, the line contribution of low charge impurity ions (C II and O II) is expected to be smaller than that found in the vertical s-FIDA spectra.

The possible contamination of the background measurement with FIDA emission induced by beam halo neutrals has also been considered. In the proposed configuration, halo neutrals may come from the present NB as well as from the upgrade heating NB (u-NB) and diagnostic NB (DNB) that are scheduled to be installed and operated in future experimental campaigns (Fig. 2). In Fig. 3(b), the distance between the beam axis and the ts-FIDA background LOS is illustrated. The background LOS passes beneath the beams ≈70 cm from the NB and 30 cm from the DNB (≈5 cm diameter and low neutral equivalent current). For comparison, the present s-FIDA background view is ≈80 cm from the NB axis in a region close to the beam entrance, where the beam has suffered small or no attenuation; no sign of relevant halo contamination has been detected so far, e.g., in beam modulation experiments. Conversely, the edge viewing LOS is closer to the u-NB. However, numerical modeling of halo spatial distribution in plasma conditions relevant to NSTX (Ref. 14) indicate that at 30 cm from the beam center, the density of halo neutrals is decayed by a factor of 10 compared to the on axis neutral density. Moreover, the minimal distance is attained at the end of the u-NB beam path, where the beam has been strongly attenuated. Hence, the halo neutrals are not expected to limit the operation of the new diagnostic.

Finally, we consider the direct D_α emission coming from excited beam neutrals. This beam emission (BE) appears in the spectrum as a strong line multiplet, corresponding to the Doppler shifted D_α lines from neutrals with different injection energies. Past s-FIDA measurements indicate that BE easily overwhelms FIDA emission. Although BE lines could, in principle, be modeled accurately, in practice, their presence in the FIDA wavelength range of interest prevents a reliable extraction of the FIDA spectrum. Figure 4 exemplifies how the BE spectrum is expected to affect the t-FIDA spectrum, for different chords. Here, a 90 keV beam is assumed, including full, 1/2, and 1/3 energy fractions. The spectroscopic system instrumental function is 0.5 nm wide (full width at half maximum), corresponding to a 100 μm entrance slit. Four impurity lines typically observed in the vertical s-FIDA spectra are included in the spectrum, with arbitrary intensity (O V: 650.1 and 660.15 nm; C II: 657.8 and 658.3 nm). For the tangential view, the BE multiplet appears on the red side wavelength for edge channels and the blue side for core channels. For chords observing the region $R=1.0–1.4$ m, covering most of outer minor radius, the BE spectrum is expected to overlap the cold D_α emission, with minimal contamination of the wavelength ranges relevant to the FIDA measurement ($E_\lambda \geq 15$ keV, $\lambda \geq 659.1$, $\lambda \leq 654$ nm). This effect, coupled with the lower perturbation expected from impurities lines, gives the t-FIDA the potential of an accurate data extraction from both red and blue Doppler shifted D_α tails. For extreme chords, covering $R<1$ m (inner midplane) and $R>1.4$ m (plasma edge), the

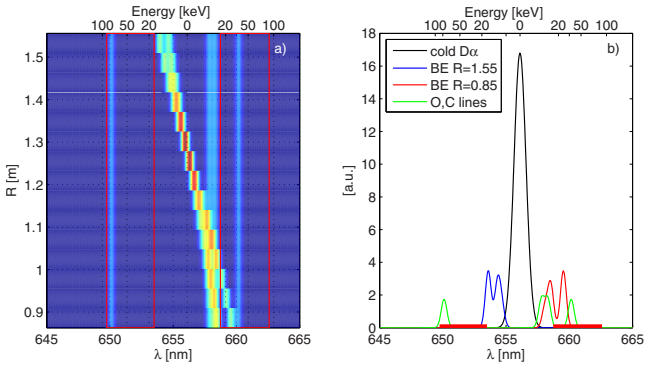

FIG. 4. (Color online) (a) Representation of the beam emission spectra from a 90 keV deuterium beam, with full, 1/2, and 1/3 energy fractions, for the 16 active LOS of ts-FIDA, as a function of the measurement radii. Four impurity lines (O V: 650.1 and 660.15 nm; C II 657.8 and 658.3 nm) are included with arbitrary intensity to indicate spectral region of eventual contamination. (b) Spectra for the innermost and outermost channels including the D_α peak. The wavelength range shown represents the expected usable range on the detector. The spectral regions corresponding to photon energies of $15 < E_\lambda < 90$ keV are delimited by vertical lines.

eventual BE contamination would restrain the analysis to reduced wavelength ranges.

IV. DIAGNOSTIC PERFORMANCE

The expected signal levels have been inferred from the performance of the present FIDA systems during plasma operation. In the proposed design, the different optical elements used (lens fibers, monochromator, and filters) have been selected with specifications close or equal to those of the present vertical system.[4] As a result, the nominal geometrical étendue of both the t-FIDA systems match approximately (within 15%) that of the present instruments.

Light detection efficiency will also be maintained; the spectroscopic measurement will rely on a back-illuminated CCD of quantum efficiency (QE)≈95% within the observed wavelength range, while for the filter measurement spare channels of the present f-FIDA, PMT array will be used (QE≈14%). During routine plasma observation, the present s-FIDA and f-FIDA signal-to-noise ratios (SNRs) are dominated by photon statistics; hence, the t-FIDA diagnostic performance may be estimated from the expected amount of input light.

Since NSTX neutral beams are vertically elongated (roughly 40 cm in height and 10 cm in width), the region of the t-FIDA LOS covered by the beam will be approximately three times smaller than in the present vertical system, with consequent relative loss of the active input signal. However, this loss is expected to be compensated by an anticipated increase of active FIDA signal by a factor >2, owing to the fact that t-FIDA will sample the distribution function at pitch values $p > 0.5$, which are characteristics of the majority of the fast ions (see Sec. I). The enhanced source of FIDA emission should permit one to attain similar SNR levels at the integration times presently used (10 ms for spectroscopic and 15 μs at 50 kHz for filter measurement).

ACKNOWLEDGMENTS

This work is supported by U.S. DOE Grant Nos. DE-FG02-06ER54867 and DE-AC02-09CH11466.

[1] Y. Luo, W. W. Heidbrink, K. H. Burrell, D. H. Kaplan, and P. Gohil, Rev. Sci. Instrum. **78**, 033505 (2007).
[2] W. W. Heidbrink, Rev. Sci. Instrum. **81**, 10D727 (2010).
[3] W. W. Heidbrink, Y. Luo, K. H. Burrell, R. W. Harvey, R. I. Pinsker, and E. Ruskov, Plasma Phys. Controlled Fusion **49**, 1457 (2007).
[4] M. Podestà, W. W. Heidbrink, R. E. Bell, and R. Feder, Rev. Sci. Instrum. **79**, 10E521 (2008).
[5] G. Taylor, R. E. Bell, J. C. Hosea, B. P. LeBlanc, C. K. Phillips, M. Podesta, E. J. Valeo, J. R. Wilson, J.-W. Ahn, G. Chen, D. L. Green, E. F. Jaeger, R. Maingi, P. M. Ryan, J. B. Wilgen, W. W. Heidbrink, D. Liu, P. T. Bonoli, T. Brecht, M. Choi, and R. W. Harvey, Phys. Plasmas **17**, 056114 (2010).
[6] E. D. Fredrickson, R. E. Bell, D. S. Darrow, G. Y. Fu, N. N. Gorelenkov, B. P. LeBlanc, S. S. Medley, J. E. Menard, H. Park, A. L. Roquemore, W. W. Heidbrink, S. A. Sabbagh, D. Stutman, K. Tritz, N. A. Crocker, S. Kubota, W. Peebles, K. C. Lee, and F. M. Levinton, Phys. Plasmas **13**, 056109 (2006).
[7] M. Podestà, W. W. Heidbrink, D. Liu, E. Ruskov, R. E. Bell, D. S. Darrow, E. D. Fredrickson, N. N. Gorelenkov, G. J. Kramer, B. P. LeBlanc, S. S. Medley, A. L. Roquemore, N. A. Crocker, S. Kubota, and H. Yuh, Phys. Plasmas **16**, 056104 (2009).
[8] The computation of diagnostic response function is addressed in the Appendix of Ref. 3.
[9] Panasonic Lumix Aspheric, G-Series, F/1.7, 20 mm.
[10] High OH pure fused silica core, 600 μm, numerical aperture: 0.4.
[11] HoloSpec F/1.8, from Kaiser Optical System.
[12] EMCCD from Princeton Instruments, model ProEM 512B, 16 bit, 10 MHz read out, frame transfer time: <0.25 ms.
[13] Hamamatsu tube, model H8711-20. Acquisition system PhotoniQ IQSP480, from Vertilon Corporation.
[14] D. Liu, "Fast-ion studies in the National Spherical Torus Experiment: Transport by instabilities and acceleration by high harmonic fast waves," Ph.D. thesis, University of California, 2009.